HHS Public Access

Author manuscript

Cardiovasc Intervent Radiol. Author manuscript; available in PMC 2015 April 13.

Published in final edited form as:

Cardiovasc Intervent Radiol. 2013 August ; 36(4): 1030–1038. doi:10.1007/s00270-012-0506-x.

Pattern of Retained Contrast on Immediate Postprocedure Computed tomography (CT) After Particle Embolization of Liver Tumors Predicts Subsequent Treatment Response

Xiaodong Wang,
Interventional Radiology Service, Department of Radiology, Memorial Sloan-Kettering Cancer Center, 1275 York Ave, Room H118, New York, NY 10065, USA. Department of Interventional Radiology, Peking University Cancer Hospital & Institute, Key Laboratory of Carcinogenesis and Translational Research (Ministry of Education), Beijing 100142, China

Joseph P. Erinjeri,
Interventional Radiology Service, Department of Radiology, Memorial Sloan-Kettering Cancer Center, 1275 York Ave, Room H118, New York, NY 10065, USA

Xiaoyu Jia,
Department of Epidemiology and Biostatistics, Memorial Sloan-Kettering Cancer Center, 1275 York Ave, New York, NY 10065, USA

Mithat Gonen,
Department of Epidemiology and Biostatistics, Memorial Sloan-Kettering Cancer Center, 1275 York Ave, New York, NY 10065, USA

Karen T. Brown,
Interventional Radiology Service, Department of Radiology, Memorial Sloan-Kettering Cancer Center, 1275 York Ave, Room H118, New York, NY 10065, USA

Constantinos T. Sofocleous,
Interventional Radiology Service, Department of Radiology, Memorial Sloan-Kettering Cancer Center, 1275 York Ave, Room H118, New York, NY 10065, USA

George I. Getrajdman,
Interventional Radiology Service, Department of Radiology, Memorial Sloan-Kettering Cancer Center, 1275 York Ave, Room H118, New York, NY 10065, USA

Lynn A. Brody,
Interventional Radiology Service, Department of Radiology, Memorial Sloan-Kettering Cancer Center, 1275 York Ave, Room H118, New York, NY 10065, USA

Raymond H. Thornton,
Interventional Radiology Service, Department of Radiology, Memorial Sloan-Kettering Cancer Center, 1275 York Ave, Room H118, New York, NY 10065, USA

Correspondence to: Stephen B. Solomon, solomons@mskcc.org.

Conflict of interest Stephen B. Solomon received a research grant from GE Healthcare (Milwaukee, WI).

Majid Maybody,
Interventional Radiology Service, Department of Radiology, Memorial Sloan-Kettering Cancer Center, 1275 York Ave, Room H118, New York, NY 10065, USA

Ann M. Covey,
Interventional Radiology Service, Department of Radiology, Memorial Sloan-Kettering Cancer Center, 1275 York Ave, Room H118, New York, NY 10065, USA

Robert H. Siegelbaum,
Interventional Radiology Service, Department of Radiology, Memorial Sloan-Kettering Cancer Center, 1275 York Ave, Room H118, New York, NY 10065, USA

William Alago, and
Interventional Radiology Service, Department of Radiology, Memorial Sloan-Kettering Cancer Center, 1275 York Ave, Room H118, New York, NY 10065, USA

Stephen B. Solomon
Interventional Radiology Service, Department of Radiology, Memorial Sloan-Kettering Cancer Center, 1275 York Ave, Room H118, New York, NY 10065, USA

Joseph P. Erinjeri: erinjerj@mskcc.org; Xiaoyu Jia: jiax@mskcc.org; Mithat Gonen: gonenm@mskcc.org; Karen T. Brown: brown6@mskcc.org; Constantinos T. Sofocleous: sofoclec@mskcc.org; George I. Getrajdman: getrajdg@mskcc.org; Lynn A. Brody: brodyl@mskcc.org; Raymond H. Thornton: throntor@mskcc.org; Majid Maybody: maybodym@mskcc.org; Ann M. Covey: covey@mskcc.org; Robert H. Siegelbaum: siegelbr@mskcc.org; William Alago: alagow@mskcc.org; Stephen B. Solomon: solomons@mskcc.org

Abstract

Purpose—To determine if the pattern of retained contrast on immediate postprocedure computed tomography (CT) after particle embolization of hepatic tumors predicts modified Response Evaluation Criteria in Solid Tumors (mRECIST) response.

Materials and Methods—This study was approved by the Institutional Review Board with a waiver of authorization. One hundred four liver tumors were embolized with spherical embolic agents (Embospheres, Bead Block, LC Bead) and polyvinyl alcohol. Noncontrast CT was performed immediately after embolization to assess contrast retention in the targeted tumors, and treatment response was assessed by mRECIST criteria on follow-up CT (average time 9.0 ± 7.7 weeks after embolization). Tumor contrast retention (TCR) was determined based on change in Hounsfield units (HUs) of the index tumors between the preprocedure and immediate postprocedure scans; vascular contrast retention (VCR) was rated; and defects in contrast retention (DCR) were also documented. The morphology of residual enhancing tumor on follow-up CT was described as partial, circumferential, or total. Association between TCR variables and tumor response were assessed using multivariate logistic regression.

Results—Of 104 hepatic tumors, 51 (49 %) tumors had complete response (CR) by mRECIST criteria; 23 (22.1 %) had partial response (PR); 21 (20.2 %) had stable disease (SD); and 9 (8.7 %) had progressive disease (PD). By multivariate analysis, TCR, VCR, and tumor size are independent predictors of CR (p = 0.02, 0.05, and 0.005 respectively). In 75 tumors, DCR was found to be an independent predictor of failure to achieve complete response (p <0.0001) by imaging criteria.

Conclusion—TCR, VCR, and DCR on immediate post-treatment CT are independent predictors of CR by mRECIST criteria.

Keywords

Clinical practice; Embolization; Embolotherapy; Liver; Hepatic

Introduction

Embolization and chemoembolization are widely applied therapies for unresectable hepatocellular carcinoma (HCC), neuroendocrine tumor liver metastases, and other hepatic metastases [1–4]. Both embolization and chemoembolization take advantage of the fact that most hepatic malignancies derive their primary blood supply from the hepatic artery rather than the portal vein. Chemoembolization exploits the preferential arterial blood supply to hepatic tumors by selectively delivering high doses of chemotherapy intraarterially to the tumor bed [5, 6]. Embolization exploits the same preferential arterial blood supply to hepatic tumors to deliver calibrated spherical embolic agents to the tumor vasculature with the intent of causing terminal vessel occlusion, thus rendering hepatic tumors ischemic and subsequently devitalized [7, 8]. Since the 1990s, some centers have used small spherical embolic agents to maximize terminal vessel blockade [9–11]. Technological improvements in particle development has allowed interventionalists using embolization to match agents to patients based on particle properties, such as size, homogeneity [9], and compressibility [12].

Visualizing distribution of lipiodol after chemoembolization by fluoroscopy or computed tomography (CT) scan ensures accurate tumor targeting, and lipiodol retention has been shown to correlate with treatment response by multiple investigators dating back to the early 1990s [13, 14]. Particle delivery is indirectly monitored during embolization by suspending particles in contrast and observing the flow of contrast into the target vessels. After embolization, there is stasis of contrast within the tumor as well as the vessels that supply the tumor. After chemoembolization, follow-up CT has been shown to detail the distribution of lipiodol within the target tumor [15]. Although lipiodol accumulation in the target tumor on postchemoembolization imaging has been shown to be predictive of therapeutic efficacy [16, 17], there has never been a report on the relevance of findings on immediate postprocedure CT after embolization without lipiodol. Given that contrast is retained by embolized tumor and is evident on immediate postembolization CT, we hypothesized that a similar predictive phenomenon could be identified after embolization without lipiodol. Because clinical therapeutic efficacy would take years to document, we chose to correlate contrast retention with radiologic findings of tumor necrosis in a pilot study. The goal of this study was to investigate whether the degree and morphology of contrast retention within the targeted tumor on immediate postprocedure CT after embolization of hepatic tumors can be used to predict subsequent modified Response Evaluation Criteria in Solid Tumors (mRECIST) response.

Materials and Methods

Subjects

A waiver of authorization was obtained from the Institutional Review Board for this retrospective study. Between February 2007 and March 2010, 63 patients underwent embolization treatment for unresectable liver tumors and were followed-up immediately by noncontrast CT scan. Embolization was chosen as treatment after discussion at a weekly multidisciplinary Hepatobiliary Disease Management Team meeting. Patients were excluded if they had undergone previous embolization or combined embolization/ablation (n = 17), had inappropriate preprocedure or follow-up imaging (n = 4), had treated tumors that did not meet mRECIST criteria for index tumor measurement (e.g., tumors <1 cm) (n = 7), or were lost to follow-up (n = 4). A total of 104 index tumors in the remaining 31 patients were included in this study. Patient demographics and tumor and embolization characteristics are listed in Table 1. The patients ranged in age from 22 to 89 years (mean 64.06 ± 15.85). There were 16 men and 15 women. Pathology included 15 cases of HCC, 13 cases of neuroendocrine liver metastases, 1 case of HCC with concomitant neuroendocrine liver metastases, 1 case of adrenocortical carcinoma, and 1 case of medullary thyroid cancer. Diagnosis of the primary malignancy was confirmed by histology or by European Association for the Study of the Liver (EASL) criteria in the case of HCC.

Embolization Technique

The technique for embolization has been previously described [10, 11]. Briefly, hepatic angiography was performed from a common femoral approach with a 4F or 5F angiographic catheter to depict the hepatic artery anatomy, location of tumors, and portal vein patency. According to operator preference, Embosphere microspheres (40–120, 100–300, or 300–500 μm; Biosphere Medical, Rockland, MA), Bead Block (100–300 μm; Biocompatibles, Farnham, UK), or LC Bead (100–300 μm; Biocompatibles) loaded with 150 mg doxorubicin were suspended in 5–10 cc nonionic contrast and used for embolization. Bland embolization was performed in 29 patients (n = 99 tumors) and drug-eluting bead embolization was performed in 2 patients (n = 5 tumors). All vessels supplying the target tumor(s) were then selectively embolized to stasis. Stasis was defined as complete cessation of antegrade flow in the vessel supplying the tumor. In 21 cases, after initial embolization with one of these agents, polyvinyl alcohol (PVA) (100 μm) was used to achieve stasis in the parent artery, which was our consistent end point of embolization. Embolization was usually performed with a microcatheter. Staged procedures were used in patients with bilobar disease or sometimes for large (>10 cm) tumors. Patients were given antiemetic and antibiotic drugs before the procedure and for at least 24 h afterward.

Tumor Response Evaluation

All patients were evaluated by preprocedure contrast-enhanced triple-phase helical CT scan within 30 days of embolization. The index tumors were identified and baseline measurements made. Immediate postprocedure non-contrast CT was performed with 20 min of completion of the last embolization procedure (after sheath removal and groin hemostasis) using a combined angio-CT system (Innova 4100/CT Lightspeed; GE Health Care). The next follow-up triphasic CT scan was performed 3–6 weeks after embolization.

Follow-up imaging with triphasic CT continued approximately every 3 months. When evidence of significant residual or new arterial enhancing tumor was identified, repeat embolization was performed.

Tumor response was assessed on the follow-up CT images according to the mRECIST criteria [18], which take lack of enhancement of the tumor into account. Unidimensional measurement of the longest diameter was recorded for each index tumor, which was selected according to mRECIST standards. The response assessment was analyzed based on each tumor's maximal response; the longest diameter of the enhancing tumor measured at follow-up was not necessarily located in the same scan plane in which the baseline diameter was measured. Response was defined as follows: complete response (CR) as disappearance of all intratumoral enhancement; partial response (PR) as >30 % decrease in diameters of enhancing tumor from baseline; progressive disease (PD) as >20 % increase in diameters of enhancing tumor from baseline; and stable disease (SD) as all other tumors. Enhancement >10 Hounsfield units (HU) on arterial phase compared with noncontrast phase was considered enhancement [19, 20]. The morphology of residual enhancing tumor was described as partial, circumferential, or total.

Contrast Retention Evaluation

Contrast retention in the index liver tumors after embolization was described by assessing tumor contrast retention (TCR), vascular contrast retention (VCR [Fig. 1]), and defects in contrast retention (DCR) on immediate post-procedure CT. TCR was based on the difference between HU of the treated tumor on immediate postembolization CT compared with preprocedure noncontrast CT. To determine TCR, the average HU of the tumor on CT with the maximum diameter was measured using an elliptical region of interest covering the majority of the tumor and subtracted from the average HU of the tumor on the immediate posttreatment scan. TCR was rated as follows: grade 0 =<30 HU increment; grade 1 = 30–60 HU increment; grade 2 = 60–120 HU increment; and grade 3 =>120 HU increment. VCR was defined as follows: grade 0 = no vessels filling around the tumor; grade 1 = Glisson's sheath filling; and grade 2 = arterial filling. DCR was defined as a peripheral defect in HU increase <30 HU that resulted in discontinuity in contrast enhancement in the periphery of the index tumor on immediate postprocedure CT. DCR was only assessed in tumors with grade 1–3 TCR because minimal tumor contrast retention seen in grade 0 TCR prevented assessment of peripheral defects in contrast retention. Assessment of contrast retention on postembolization CT and assessment of tumor response were made independently in a blinded fashion.

Statistics

Univariate analyses for response as outcome (CR vs. no CR) was performed using logistic regression on 104 index tumors for each contrast retention and patient/tumor characteristic variable. The correlation between TCR and VCR was assessed using Kendall's tau correlation coefficient. To identify the clinical factors jointly associated with response, a backward variable selection procedure was applied on all variables except DCR (not evaluable for patients with TCR grade 0) and catheter type (too sparse) with the variable retaining criteria of $p \leq 0.05$.

To examine whether high contrast retention after embolization is desirable in both the target tumor (TCR) and the vasculature (VCR), three sets of multivariate models were developed each with TCR alone, VCR alone, and TCR + VCR, adjusting for other statistically significant clinical factors identified using the variable selection procedure. Concordance index (C-index) was used to evaluate the models' discriminatory ability. C-index of 0.5 indicates no discrimination, and 1 indicates perfect discrimination. In addition, a separate model was built on the subset of patients with measures on defect of tumor contrast retention (DCR). Dependency between lesions in the same patient was accounted for by using generalized estimation equations. All analyses were performed in SAS (version 9.2; SAS, Cary, NC).

Results

During the investigation period, a total of 31 patients with 104 index tumors were treated in 32 embolization sessions. Tumor characteristics, including histopathology, size, density, location, and distribution, and the microspheres used for embolization are listed in Table 1. Average time of follow-up CT scan used to assess mRECIST response was 9.0 ± 7.7 weeks after embolization (range 4–36).

Contrast Retention and Tumor Response

Total necrosis by imaging (CR) was 6.9, 51.9, 70, and 77.8 % for TCR grade 0, 1, 2, and 3, respectively (Table 2, Fig. 2) and 22, 50, and 76.9 for VCR grade 0, 1, and 2, respectively (Figs. 3, 4). DCR was assessed in the 75 of 104 tumors in which TCR was greater than grade 0; DCR could not be assessed in tumors with less robust contrast retention. CR rate was 90.6 % for tumors without DCR and 5.6 % when DCR was present. Data stratification by DCR showed that in the 57 tumors without DCR, CR was 66.7, 91.3, and 100 % for TCR 1, 2, and 3, respectively. Not surprisingly, TCR and VCR were correlated (Kendall's tau 0.48 p <0.0001) (Table 3). Tumors with TCR grade 1–3 were more often accompanied with Glisson's sheath or arterial filling around the index tumor than those with TCR grade 0. We examined the follow-up CT of patients with tumors that exhibited DCR to determine the morphology of the residual enhancing tumor on follow-up (Table 4). Tumors with TCR grade 0 on postprocedure CT showed enhancing residual disease in the corresponding area on follow-up CT (22 of 29 tumors). In tumors where DCR was present on immediate postprocedure CT, the morphology of the residual enhancing tumor seen on follow-up CT was focal in 7 of 18 tumors (Fig. 5) and circumferential in 8 of 18 tumors. Tumors without DCR on immediate postprocedure CT tended to result in complete lack of enhancement and radiologic findings of complete necrosis on follow-up CT (48 of 57 tumors).

Predictors of CR

To determine the patient, tumor, and contrast retention variables associated with CR, univariate analyses were performed (Table 5). TCR, VCR, and DCR were associated with CR in univariate analyses. Among other clinical factors, only tumor size and location were useful for predicting CR in univariate analysis.

Multivariate analysis (Table 6) showed that after adjusting for tumor size, TCR was strongly associated with radiologic CR, whereas tumors with lower grades of TCR were less likely to achieve this (overall $p = 0.009$); e.g., grade 2 vs. 3 TCR (OR 0.51; 95 % CI 0.18–1.42); grade 1 vs. 3 TCR (OR 0.27; 95 % CI 0.07–1.12); and grade 0 vs. 3 TCR (OR 0.01; 95 % CI 0–0.10). Similarly, after controlling for tumor size, VCR was associated with radiologic CR. Lower grades of VCR were also less likely to achieve this (second panel, Table 6). Because TCR and VCR were correlated, we created a joint multivariate model including both TCR and VCR as independent factors. Slightly attenuated ordinal effects remained for TCR and VCR in the multivariate model where both were included (third panel in Table 6). Nonetheless, the overall p value was 0.02 and 0.05 for TCR and VCR, respectively, in the joint model, suggesting that high contrast retention in both target tumor and vasculature is predictive of achieving radiologic CR. The TCR model had a higher concordance index than the VCR model: 0.85 vs. 0.79. The joint model had an even higher concordance index of 0.87. The increase of prediction accuracy was 0.06 from the VCR model to the TCR model and a less discernible 0.018 from the TCR model to the joint model. The results suggest that it is desirable to reach the highest grade of contrast retention in both target tumor and vasculature because the joint model further enhances prediction accuracy of a radiologic CR. Among 75 tumors where DCR could be measured, multivariate analysis (last panel in Table 6) suggested that both DCR and TCR were independent predictors of achieving a complete radiologic response (OR 0.005 [$p < 0.0001$] and OR 0.11 [$p < 0.02$], respectively).

Discussion

Predicting the results of embolization at the time of treatment can be challenging. In this study, using multivariate analysis we found that the imaging findings of TCR, VCR, and DCR of the index tumor(s) on immediate postprocedure CT embolization are all independent predictors of a radiologic CR on follow-up CT imaging using mRECIST criteria. TCR and VCR were positive predictors of mRE-CIST CR; DCR was a negative predictor of CR. Achieving at least grade 1 TCR without DCR resulted in an 84.2 % mRECIST CR rate; achieving grade 2 TCR without DCR resulted in a 94.4 % mRECIST CR rate. Based on our findings, to maximize the likelihood of CR per mRECIST criteria after embolization, the end point of embolization should be maximal contrast retention in both the tumor and feeding vasculature. Of note, our data suggest that an end point of embolization that aims to fill the tumor without filling its feeding vasculature would fail to take advantage of the independent increases in CR afforded by employing vascular stasis as the end point of embolization, which maximizes both VCR and TCR.

In this study, DCR was a reliable predictor of recurrent disease. Our analysis of the residual tumor morphology provides some evidence for the etiology of treatment failures after embolization. Not surprisingly, we observed that less robust contrast retention in the index tumor on immediate follow-up C, tends to result in persistent enhancement of the entire tumor on subsequent follow-up CT. On follow-up imaging, tumors without DCR tend to result in total lack of enhancement (complete radiologic necrosis), whereas tumors with DCR tend to result in partial or circumferential residual enhancing tumor with the area of DCR corresponding to the region of subsequent recurrent tumor in 75 % (22 of 29) of patients.

Performing CT before the patient leaves the angiography suite enables the operator to adjust the treatment in real time. For example, if DCR is identified, other blood vessels (hepatic or nonhepatic) can be interrogated to determine if they supply the tumor, or ablation of the underembolized portion of the tumor could be performed. Spasm resulting from guidewire or catheter manipulation in a feeding vessel is another potential cause of a defect in contrast retention and embolization failure [21]. This could be considered at the time of treatment, if DCR is identified, and potentially reversed with vasodilators.

The findings in this study may also be relevant to chemoembolization with drug-eluting bead. Like embolization, drug-eluting bead embolization relies on the suspension of particles in contrast for treatment monitoring [22, 23]. Based on the results of this study, we suspect that TCR, VCR, and DCR on postembolization helical or cone-beam CT [15] after drug-eluting bead embolization might also correlate with radiologic findings of necrosis. Performing this evaluation immediately after embolization when the patient is on the operating table enables the operator to adjust the treatment before the patient leaves the angiography suite.

To assess contrast retention at the time of embolization using the findings described in this study, a combined angio-CT system or cone-beam CT is needed so that CT can be performed without requiring the patient to move from the fluoroscopy suite to a dedicated CT room. This adds approximately 5–10 min to the procedure time and 500 mrem to the procedure dose. Multiple investigators have documented the advantage of intraprocedural CT hepatic angiography for prospectively identifying vessels supplying the target tumor [24, 25].

This study has several limitations. Tumor response is based on follow-up CT imaging rather than histopathology. Lack of tumor enhancement on contrast-enhanced CT has been correlated with pathologic necrosis [18], and the presence of arterial enhancement on CT is considered evidence of tumor viability [16]. Because we do not have long-term follow-up on this cohort of patients with various primary tumors, we cannot make claims regarding contrast retention and patient survival. We do plan to correlate TCR, VCR and DCR in future prospective studies with patient clinical outcome. Contrast retention in tumors and the corresponding arteries after particle embolization is temporary, and the kinetics of contrast wash-out is unknown. In this retrospective study, CT was performed within 20 min of conclusion of the final embolization. When multiple vessels were treated, it is quite possible that contrast begins to wash out from the tumors and vessels treated earlier in the procedure. It is conceivable that our few discrepant cases in which CR was achieved despite TCR grade 0 (6.9 %) or VCR grade 0 (22 %) are due to prolonged delay between completion of embolization of these tumors and immediate postembolization CT scan. Finally, in this retrospective study, a variety of particle sizes and types were used, and the tumor pathology was not uniform; the majority of tumors were treated with bland embolization. This raises the question of the general applicability of these results.

Conclusion

After embolization, TCR, VCR, and DCR on immediate postembolization CT are independent predictors of radiologic complete response. Moderate to marked tumor contrast retention with Glisson's sheath filling or arterial filling without defect in contrast retention is an ideal end point of embolization. These findings suggest that, when available, CT (helical or cone-beam) performed immediately after embolization provides added clinical value. A defect in contrast retention should prompt careful review of preprocedure multiphasic and DSA imaging. This review could identify other vessels supplying the tumor that have not been treated or vessels that were previously in spasm, thus precluding delivery of embolic to the tumor. Whether complete treatment of the target tumor will affect survival remains to be investigated.

References

1. Dhanasekaran R, Kooby DA, Staley CA, et al. Comparison of conventional transarterial chemoembolization (TACE) and chemoembolization with doxorubicin drug eluting beads (DEB) for unresectable hepatocelluar carcinoma (HCC). J Surg Oncol. 2010; 101(6):476–480. [PubMed: 20213741]
2. Kim JH, Yoon HK, Ko GY, et al. Nonresectable combined hepatocellular carcinoma and cholangiocarcinoma: analysis of the response and prognostic factors after transcatheter arterial chemoembolization. Radiology. 2010; 255(1):270–277. [PubMed: 20308463]
3. Nazario J, Gupta S. Transarterial liver-directed therapies of neuroendocrine hepatic metastases. Semin Oncol. 2010; 37(2):118–126. [PubMed: 20494704]
4. Malagari K, Pomoni M, Spyridopoulos TN, et al. Safety profile of sequential transcatheter chemoembolization with DC Bead: results of 237 hepatocellular carcinoma (HCC) patients. Cardiovasc Intervent Radiol. 2011; 34(4):774–785. [PubMed: 21184228]
5. Liapi E, Geschwind JF. Chemoembolization for primary and metastatic liver cancer. Cancer J. 2010; 16(2):156–162. [PubMed: 20404613]
6. Lencioni R, de Baere T, Burrel M, et al. Transcatheter treatment of hepatocellular carcinoma with doxorubicin-loaded DC Bead (DEBDOX): technical recommendations. Cardiovasc Intervent Radiol. 2011; 35:980–985. [PubMed: 22009576]
7. Tadavarthy SM, Knight L, Ovitt TW, et al. Therapeutic transcatheter arterial embolization. Radiology. 1974; 112(1):13–16. [PubMed: 4545553]
8. Allison DJ, Modlin IM, Jenkins WJ. Treatment of carcinoid liver metastases by hepatic-artery embolisation. Lancet. 1977; 2(8052–8053):1323–1325. [PubMed: 74732]
9. Bonomo G, Pedicini V, Monfardini L, et al. Bland embolization in patients with unresectable hepatocellular carcinoma using precise, tightly size-calibrated, anti-inflammatory micro-particles: first clinical experience and one-year follow-up. Cardiovasc Intervent Radiol. 2010; 33(3):552–559. [PubMed: 19957182]
10. Covey AM, Maluccio MA, Schubert J, et al. Particle embolization of recurrent hepatocellular carcinoma after hepatectomy. Cancer. 2006; 106(10):2181–2189. [PubMed: 16596622]
11. Maluccio MA, Covey AM, Porat LB, et al. Transcatheter arterial embolization with only particles for the treatment of un-resectable hepatocellular carcinoma. J Vasc Interv Radiol. 2008; 19(6): 862–869. [PubMed: 18503900]
12. Lewis AL, Adams C, Busby W, et al. Comparative in vitro evaluation of microspherical embolisation agents. J Mater Sci Mater Med. 2006; 17(12):1193–1204. [PubMed: 17143749]
13. Uchida H, Matsuo N, Nishimine K, et al. Transcatheter arterial embolization for hepatoma with lipiodol—Hepatic arterial and segmental use. Semin Intervent Radiol. 1993; 10(1):19–26.
14. Choi BI, Kim HC, Han JK, et al. Therapeutic effect of transcatheter oily chemoembolization therapy for encapsulated nodular hepatocellular carcinoma: cT and pathological findings. Radiology. 1992; 182(3):709–713. [PubMed: 1311116]

15. Tognolini A, Louie JD, Hwang GL, et al. Utility of C-arm CT in patients with hepatocellular carcinoma undergoing transhepatic arterial chemoembolization. J Vasc Interv Radiol. 2010; 21(3): 339–347. [PubMed: 20133156]
16. Vogl TJ, Trapp M, Schroeder H, et al. Transarterial chemoembolization for hepatocellular carcinoma: volumetric and morphologic CT criteria for assessment of prognosis and therapeutic success—Results from a liver transplantation center. Radiology. 2000; 214(2):349–357. [PubMed: 10671580]
17. Takayasu K, Muramatsu Y, Maeda T, et al. Targeted transarterial oily chemoembolization for small foci of hepato-cellular carcinoma using a unified helical CT and angiography system: analysis of factors affecting local recurrence and survival rates. AJR Am J Roentgenol. 2001; 176(3):681–688. [PubMed: 11222205]
18. Lencioni R, Llovet JM. Modified RECIST (mRECIST) assessment for hepatocellular carcinoma. Semin Liver Dis. 2010; 30(1):52–60. [PubMed: 20175033]
19. Berber E, Foroutani A, Garland AM, et al. Use of CT Hounsfield unit density to identify ablated tumor after laparoscopic radiofrequency ablation of hepatic tumors. Surg Endosc. 2000; 14(9): 799–804. [PubMed: 11000357]
20. Herber S, Biesterfeld S, Franz U, et al. Correlation of multislice CT and histomorphology in HCC following TACE: predictors of outcome. Cardiovasc Intervent Radiol. 2008; 31(4):768–777. [PubMed: 18196335]
21. Fujita T, Ito K, Tanabe M, et al. Iodized oil accumulation in hypervascular hepatocellular carcinoma after transcatheter arterial chemoembolization: comparison of imaging findings with CT during hepatic arteriography. J Vasc Interv Radiol. 2008; 19(3):333–341. [PubMed: 18295691]
22. Kloeckner R, Otto G, Biesterfeld S, et al. MDCT versus MRI assessment of tumor response after transarterial chemo-embolization for the treatment of hepatocellular carcinoma. Cardiovasc Intervent Radiol. 2010; 33(3):532–540. [PubMed: 19847482]
23. Moschouris H, Malagari K, Papadaki MG, et al. Contrast-enhanced ultrasonography of hepatocellular carcinoma after chemoembolisation using drug-eluting beads: a pilot study focused on sustained tumor necrosis. Cardiovasc Intervent Radiol. 2010; 33(5):1022–1027. [PubMed: 20101403]
24. Sze DY, Razavi MK, So SK, et al. Impact of multidetector CT hepatic arteriography on the planning of chemoembolization treatment of hepatocellular carcinoma. AJR Am J Roentgenol. 2001; 177(6):1339–1345. [PubMed: 11717079]
25. Iwazawa J, Ohue S, Mitani T, et al. Identifying feeding arteries during TACE of hepatic tumors: comparison of C-arm CT and digital subtraction angiography. AJR Am J Roentgenol. 2009; 192(4):1057–1063. [PubMed: 19304714]

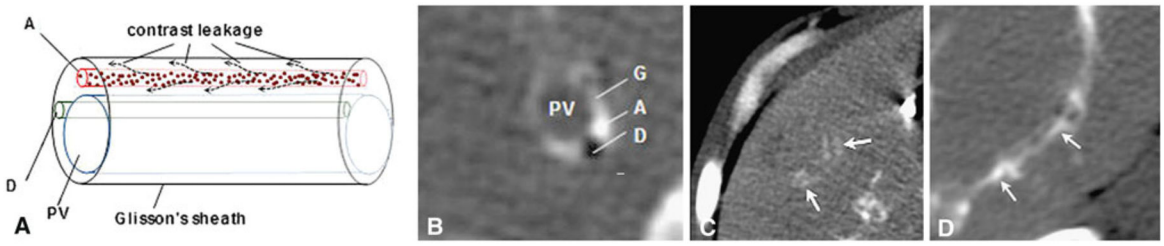

Fig. 1.

A Diagram of Glisson's sheath, and theorized contrast leakage from the arterioles with **B** cross-sectional image. **C** Glisson's sheath filling (arrows) = VCR grade 1. **D** Arterial filling (arrows) = VCR grade 2. *PV* portal vein, *A* artery, *D* bile duct, *G* Glisson's sheath

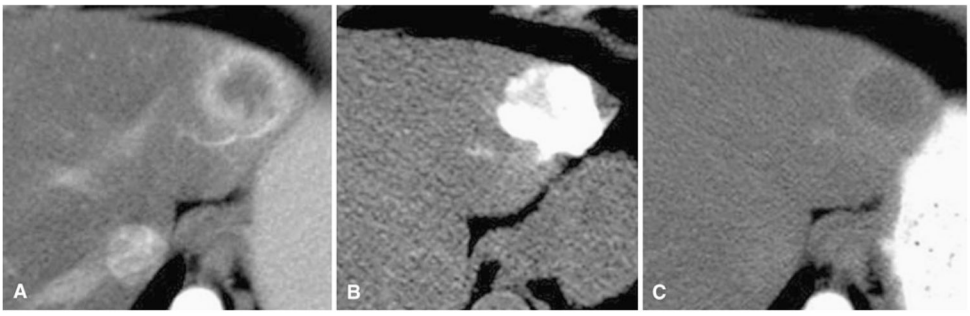

Fig. 2.

A 62-year-old woman with metastatic thyroid cancer to liver. **A** Arterial phase preprocedure contrast-enhanced CT shows index tumor in left liver. **B** Immediate postembolization CT shows grade 3 TCR with grade 0 VCR without DCR. **C** Follow-up contrast-enhanced CT shows CR by mRECIST criteria

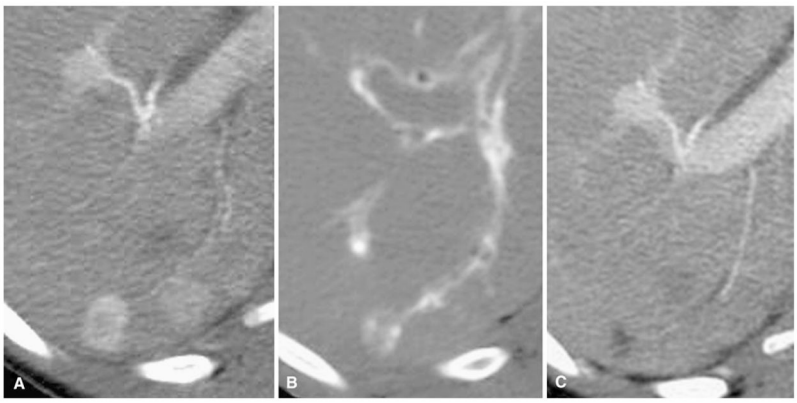

Fig. 3.

A 44-year-old woman with metastatic neurocrine tumor to liver. **A** Arterial phase preprocedure contrast-enhanced CT shows index tumor in the posterior segment of the right lobe. **B** Immediate postembolization CT shows grade 2 TCR with filling arteries entering tumor (grade 2 VCR) without DCR. **C** Follow-up contrast-enhanced CT shows CR by mRECIST criteria

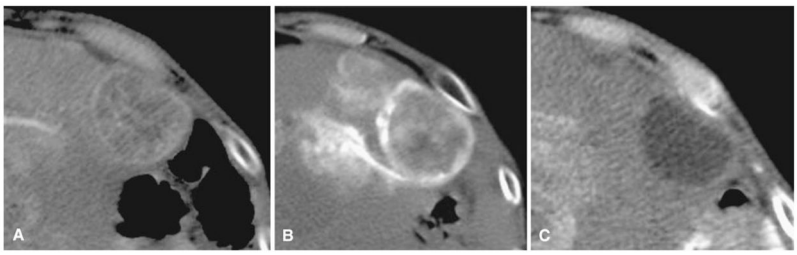

Fig. 4.

22-year-old woman with metastatic neuroendocrine tumor to liver. **A** Arterial phase preprocedure contrast enhanced CT shows index tumor in left lobe. **B** Immediate postembolization CT shows grade 1 TCR with grade 2 VCR without DCR. **C** Followup contrast enhanced CT shows CR by mRECIST criteria

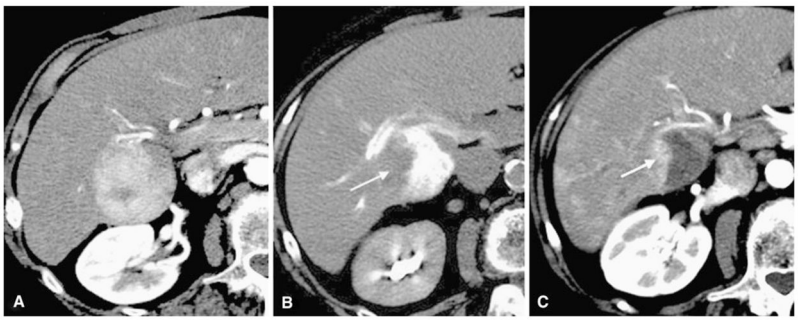

Fig. 5.

An 84-year-old woman with hepatocellular carcinoma. **A** Arterial phase preprocedure contrast-enhanced CT shows index tumor in segments V and VI. **B** Immediate postembolization CT shows DCR on the right side of the tumor (*arrow*) despite grade 2 TCR and grade 2 VCR. **C** Follow-up contrast-enhanced CT shows partial residual enhancing tumor morphology (*arrow*) corresponding to the contrast retention defect

Table 1

Tumor and treatments characteristics

Characteristic	
Histopathology (%)	
HCC	21 (20.2)
Neuroendocrine	77 (74)
Adrenocortical carcinoma	5 (4.8)
Medullary thyroid cancer	1 (1)
Baseline (%) tumor density (HU)	43.77 ± 6.10
<45	53 (51)
>45	51 (49)
Location (%)	
Segment 1	6 (5.8)
Segment 2	12 (11.5)
Segment 3	13 (12.5)
Segment 4	17 (16.3)
Segment 5	6 (5.8)
Segment 6	18 (17.3)
Segment 7	12 (11.5)
Segment 8	14 (13.5)
Cross–multiple segment	6 (5.8)
Distribution (%)	
Multifocal	93 (89.4)
Unifocal	11 (10.6)
Particles (%)	
Embosphere	
40–120 μm	23 (22.1)
100–300 μm	51 (49)
300–500 & 500–700 (μm)	1 (1)
Bead Block (100–300 μm)	3 (2.9)
Embosphere & PVA (100 μm)	16 (15.4)
Bead Block & PVA	5 (4.8)
LC Bead (100–300 μm) & Bead Block	5 (4.8)
Catheter for TAE (%)	
Microcatheter	101 (97.1)
Diagnostic catheter	3 (2.9)
Index (range) tumor nos./patient	3.35 ± 3.10 (1–14)
Size (range) mean + SD (mm)	35.81 ± 26.38 (10.04–165)
<30 mm	59 (56.7)
>30 mm	45 (43.3)

Table 2

Contrast retention variables and tumor response

Variable	Response			
	PD	SD	PR	CR
TCR (%)				
Grade 0 (*n* = 29)	8	13	6	2 (6.9)
Grade 1 (*n* = 27)	1	4	8	14 (51.9)
Grade 2 (*n* = 30)	0	2	7	21 (70.0)
Grade 3 (*n* = 18)	0	2	2	14 (77.8)
TCR (no DCR [%])				
Grade 1 (*n* = 21)	0	4	3	14 (66.7)
Grade 2 (*n* = 23)	0	0	2	21 (91.3)
Grade 3 (*n* = 13)	0	0	0	13 (100)
VCR (%)				
Grade 0 (*n* = 41)	7	13	12	9 (22.0)
Grade 1 (*n* = 24)	2	7	3	12 (50.0)
Grade 2 (*n* = 39)	0	1	8	30 (76.9)
DCR (%)				
No (*n* = 57)	0	4	5	48 (90.6)
Yes (*n* = 18)	1	4	12	1 (5.6)

Table 3

Correlation between TCR and VCR

	TCR					
	Grade 0	**Grade 1**	**Grade 2**	**Grade 3**	**Kendall's tau**	***p***
VCR					0.48	0.0001
Grade 0 (*n* = 41)	21	15	4	1		
Grade 1 (*n* = 24)	5	4	11	4		
Grade 2 (*n* = 39)	3	8	15	13		

Table 4

Relationship between DCR status and morphology of residual tumor

	No residual tumor	Residual tumor		
		Partial	Circumferential	Total
TCR 0	2	4	1	22
TCR 1–3				
DCR (yes)	1	7	8	3
DCR (no)	48	3	2	4

Table 5

Univariate analysis of predictors of CR

Factors	OR	95 % CI	*p*
Patient and tumor variables			
Sex M vs. F	1	(0.34, 2.96)	1
Size >3 vs. <3 cm	0.27	(0.11, 0.69)	0.005
Pathology			0.62
Neuroendocrine vs. HCC	1.76	(0.51, 6.00)	
Others vs. HCC	1.63	(0.41, 6.53)	
Baseline tumor density			0.75
>45 vs. <45 HU	0.86	(0.33, 2.23)	
Location			0.05
Left vs. right	0.79	(0.21, 2.90)	
Multisegment vs. right	0.16	(0.02, 1.38)	
Caudate vs. right	0.16	(0.02, 1.35)	
Caudate vs. others[a]	0.019	(0.03, 1.37)	0.065
Particles			0.58
100–300 vs. 40–120 embosphere (μm)	0.45	(0.10, 1.95)	
Others vs. 40–120 embosphere (μm)	0.73	(0.14, 3.77)	
Unifocal vs. multifocal	0.35	(0.08, 1.50)	0.15
Contrast retention variables			
TCR			0.012
0 vs. 3	0.02	(0, 0.12)	
1 vs. 3	0.31	(0.08, 1.19)	
2 vs. 3	0.67	(0.23, 1.88)	
VCR			0.0055
0 vs. 2	0.08	(0.03, 0.24)	
1 vs. 2	0.3	(0.1, 0.93)	
DCR (among 75 available tumors)			
No vs. yes	90.6	(8.02, 1,025)	0.0006

[a]Location was regrouped into caudate versus others to address this specific clinic question

Table 6

Multivariate models of predictors of CR

Model	OR	95 % CI	*p*	Model C-index
TCR model (*N* = 104)				0.85
TCR			0.01	
TCR 0 vs. 3	0.01	(0, 0.10)		
TCR 1 vs. 3	0.27	(0.07, 1.12)		
TCR 2 vs. 3	0.51	(0.18, 1.42)		
Size >3 vs. <3 cm	0.19	(0.06, 0.54)	0.005	
VCR model (*N* = 104)				0.79
VCR			0.006	
VCR 0 vs. 2	0.086	(0.03, 0.26)		
VCR 1 vs. 2	0.32	(0.12, 0.86)		
Size >3 vs. <3 cm	0.27	(0.11, 0.70)	0.01	
TCR + VCR model (*N* = 104)				0.87
TCR			0.02	
TCR 0 vs. 3	0.03	(0, 0.21)		
TCR 1 vs. 3	0.54	(0.14, 2.06)		
TCR 2 vs. 3	0.69	(0.26, 1.87)		
VCR				
VCR 0 vs. 2	0.21	(0.10, 0.47)	0.05	
VCR 1 vs. 2	0.36	(0.12, 1.04)		
Size >3 vs. <3 cm	0.20	(0.06, 0.61)	0.005	
DCR model (*N* = 75)				
DCR yes vs. no	0.005	(0, 0.04)	<0.0001	
TCR 1 vs. 2 or 3	0.11	(0.02, 0.72)	0.02	